ARTICLE

Biomimetic Reusable Microfluidic Reactors with Physically-Immobilized RuBisCO for Glucose Precursor Production†

Received 00th January 20xx,
Accepted 00th January 20xx

DOI: 10.1039/x0xx00000x

Yujiao Zhu[a, b], Qingming Chen[c], Chi Chung Tsoi[a], Xiaowen Huang[d], Abdel El Abed[e], Kangning Ren*[b], Shao-Yuan Leu[f] and Xuming Zhang*[a]

Chloroplast of plants is a natural microfluidic reactor for natural photosynthesis, in which, the multi-enzymatic Calvin cycle is the key. In chloroplast, the Calvin cycle enzymes are reportedly attached to thylakoid membrane by physical interactions. To mimic this process, we physically immobilized the first enzyme of Calvin cycle, D-ribulose-1,5-bisphosphate carboxylase/oxygenase (RuBisCO), into microfluidic reactors by injecting 2 μg μL^{-1} of RuBisCO for 4 h and demonstrated the successful production of glucose precursor, 3-phosphoglycereate, at 0.145 ± 0.008 nmol min^{-1}. Hydrophobic interactions play an important role in the physical immobilization, making the process simple and fast. The physical immobilization presents a 5.7-fold thermal stability as compared to the free RuBisCO, and shows the performances inferior but close to the chemical immobilization in enzyme kinetics, production rate and stability. Although the reactors can only retain 40% of the initial activity after 10 cycles of reusing, the physical immobilization has an interestingly special feature that the enzyme can be desorbed to refresh the reactor for new immobilization. Experiments show that > 95% activity can be restored after 5 cycles of refreshing. With the merits of reusing and refreshing, up to 5 mL of 3-PGA can be produced by continuously injecting the reactant mixture with great sustainability and cost-effectiveness. The reactors are also scaled out to two and six parallel reactors as a proof-of-concept of large-scale synthesis. The physical immobilization in microfluidic reactors is highly suitable for the multi-enzymatic, cascaded reactions in Calvin cycle, and facilitates the future study of artificial synthesis of glucose.

1. Introduction

Plants use a process called natural photosynthesis (NPS) in their chloroplasts to make food. Glucose is the direct product of NPS and the basic material to synthesize other substances such as starch and cellulose. However, D-ribulose-1,5-bisphosphate carboxylase/oxygenase (RuBisCO, EC 4.1.1.39), as the key enzyme of NPS, has low activity and poor specificity, seriously limiting the energy efficiency of food production to only ~1%.[1] In addition, humans have long been struggling with food shortages due to extreme weather, population explosion and land resource exhaustion. Therefore, scientific solutions are in urgent need for massive food production using man-made materials and engineered reactors. It is well-known that Calvin cycle enzymes are bound to the thylakoid membranes in the stroma of natural plants.[2-5] Efforts have been devoted to immobilizing and concentrating RuBisCO into man-made structures with improved activity and selectivity implementing the biomimetic Calvin cycle process.[6-9] For decades, due to the potentials of high efficiency and simplicity, artificial photosynthesis (APS) has been explored to substitute the NPS for the production of energy-rich chemicals.[10] It generally uses semiconductors or engineered chloroplasts to capture light for water splitting, biofuel production and photocatalytic cofactor regeneration.[11-15] However, most prior studies were conducted in bulk reactors, different from the fluid-filled chloroplasts which could be regarded as natural microfluidic reactors. In a previous study, we followed the concept of APS to artificially synthesize the glucose precursor, 3-phosphoglycereate (3-PGA), by using *phase 1* of Calvin cycle with microfluidics to mimic the chloroplasts.[16] RuBisCO was chemically immobilized into polydimethylsiloxane (PDMS)-made microfluidic reactors to convert ribulose-1,5-bisphophate (RuBP) and carbon dioxide (CO_2) into 3-PGA. The combination of microfluidics and chemical immobilization in biocatalysis offers great cost-effectiveness, sustainability, reusability and stability.[17] The advantages of easy control of reaction condition, easy separation and collection of the products, avoidance of inhibition by the accumulated products, and continuous production using a small amount of enzyme are also obvious.[16,

[a] *Department of Applied Physics, The Hong Kong Polytechnic University, Hong Kong, 999077, P. R. China.*
* *E-mails: apzhang@polyu.edu.hk; kangningren@hkbu.edu.hk*
[b] *Department of Chemistry, Hong Kong Baptist University, Hong Kong, 999077, P. R. China*
[c] *School of Microelectronics Science and Technology, Sun Yat-sen University, Zhuhai, 519082, P. R. China.*
[d] *State Key Laboratory of Biobased Material and Green Papermaking; Shandong Provincial Key Laboratory of Microbial Engineering, Department of Bioengineering, Qilu University of Technology (Shandong Academy of Sciences), Jinan, 250353, P. R. China.*
[e] *Laboratoire Lumière Matière et Interfaces (LuMIn), Institut d'Alembert, ENS Paris Saclay, CentraleSupélec, CNRS, Université Paris-Saclay, 4 avenue des Sciences, 91190 Gif-sur-Yvette, France.*
[f] *Department of Civil and Environmental Engineering, Hong Kong Polytechnic University, Hong Kong, 999077, P. R. China.*
† *Electronic Supplementary Information (ESI) available. See DOI: 10.1039/x0xx00000x*

[18] Nevertheless, the chemical immobilization requires additional linkers, which may contaminate the products and need complicated preparation.[19] In addition, Calvin cycle enzymes were reported to associated with the thylakoid membrane by physical interactions rather than specific chemical interaction.[2] To mimic the physical interaction environment of enzyme in nature, here we examine physical immobilization by directly adsorbing RuBisCO on the inner surfaces of PDMS microfluidic reactors, and then verify its feasibility in the 3-PGA production.

PDMS is a popular fabrication material for microfluidic devices of biological applications. It has many superior characteristics such as easy fabrication, optical transparency, biocompatibility, and favourable thermal and electrical properties.[20] One of the most notable features of PDMS is its hydrophobicity (contact angle ~ 110°), allowing non-specific adsorption of various molecules.[21] It can also become hydrophilic after some surface treatment such as oxygen plasma bombardment, UV oxidation, chemical modification or dynamic coating.[22, 23] The plasma treatment is the most popular method for hydrophilic improvement without introducing additional chemical bonds.[24-26] Compared with the hydrophilic surfaces, hydrophobic surfaces can adsorb more enzymes thanks to the hydrophobic interactions.[27-30] The adsorbed enzymes on hydrophobic surfaces also present higher activity and excellent activity retention.[31, 32]

For the physical adsorption in PDMS microfluidic reactors, enzyme is bound to supports via physical attractive forces, such as van der Waals forces, hydrogen bonds, charge interactions or hydrophobic interactions.[18] Compared with the chemical immobilization, it is mild, simple, and relatively green and chemical-free (see Figure 1(a)).[33] The immobilization procedure is significantly simplified. It may also retain high activity with low cost.[34] However, the physical bonding forces are usually weak and vulnerable to the buffer conditions, like pH, temperature, and ionic strength.[35] This presents to be a severe drawback in many cases since the enzymes may leach and contaminate the substrate.[36] Nevertheless, it could also be favourable in some other cases. For instance, it could adsorb multiple enzymes onto the same substrate in a single immobilization step or successive steps; and the physical bonding between the enzyme and the supports is usually reversible and thus the enzyme can be desorbed in a controlled manner to recycle the supports with newly immobilized enzymes.[37, 38] These are special merits of physical immobilization, which make it particularly suitable for multi-enzymatic reactions (e.g., Calvin cycle) in a green and sustainable way.

In this work, the pristine PDMS and the plasma-treated PDMS are both used in the PDMS microfluidic reactors (PMRs) for RuBisCO immobilization. Their performances are compared in terms of the protein loading capacity and the 3-PGA production. Optimal conditions are then investigated by adjusting the RuBisCO concentration, the flow rate of immobilization and the immobilization time for the fabrication of RuBisCO-immobilized PDMS-based microfluidic reactors (RI-PMRs). Their feasibility and reusability are also tested under the optimal condition. Afterwards, the special feature of refreshing and recycling of the RI-PMRs is investigated by repeated acid buffer washing and new enzyme immobilization. Continuous production is achieved by taking advantage of the reusing and refreshing. This merit also makes it possible to replace and renew the immobilized

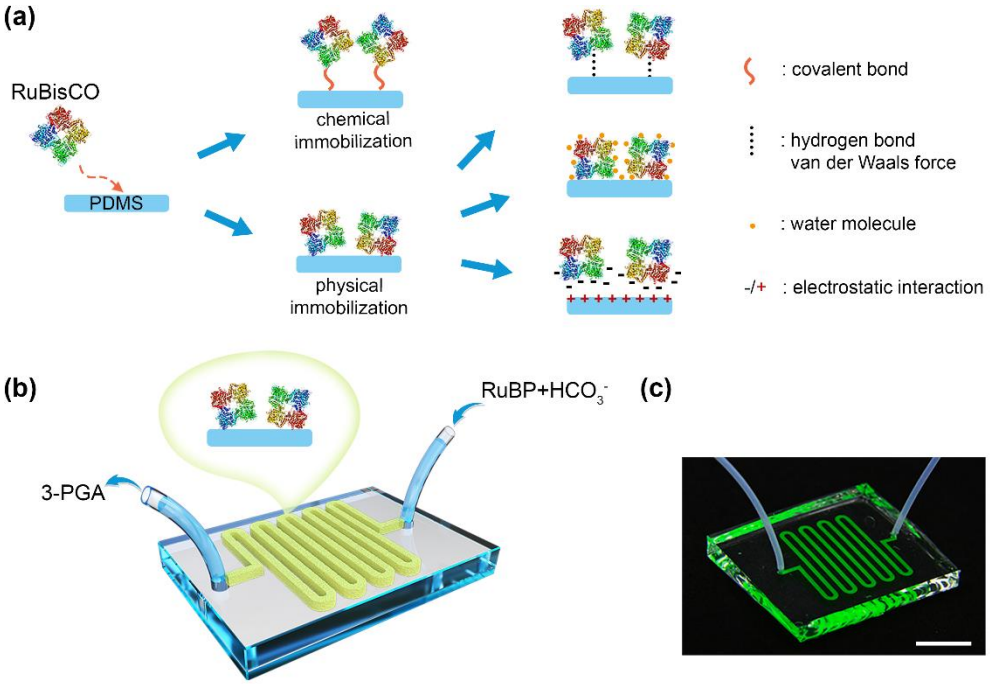

Figure 1. Schematics of the RuBisCO-immobilized PDMS-based microfluidic reactor (RI-PMRs). (a) Comparison of the procedures of chemical immobilization and physical immobilization for RuBisCO. For the chemical immobilization, the interactions between enzyme and supports are mainly covalent bonds. For the physical adsorption, the interactions include hydrogen bonds, van der Waals forces, hydrophobic interactions, and electrostatic interactions. (b) 3D diagram and (c) the photograph of the RI-PMRs. RuBP and HCO_3^- are injected into the inlet and 3-PGA is collected from the outlet. The scale bar of the photograph is 1 cm.

enzymes and then to perform different reactions by reusing the same reactor. At last, scaling out the reactor for one to two and six parallel reactors is conducted as a proof-of-concept for large-scale synthesis of 3-PGA. With the new attempt, this work consolidates the foundation of artificial synthesis of basic food materials using microfluidics by mimicking the NPS in chloroplasts, which supplements our previous study on chemical immobilization so as to build up comprehensive technical bases for the immobilization of enzymes in microfluidic reactors for APS. One valuable step is advanced to the relief of food crisis and the future space colonization.

2. Experimental section

2.1. Chemicals and regents

The reaction buffer (pH 8.0) used for enzyme assay consisted of 0.1 M tris(hydroxymethyl)aminomethane buffer (Tris-HCl, pH 8.0, Beijing Solarbio Technology Co., Ltd., Beijing), 5 mM magnesium chloride hexahydrate ($MgCl_2 \times 6H_2O$, AR, Sinopharm Chemical Reagent Co., Ltd, Shanghai), 66 mM potassium bicarbonate ($KHCO_3$, AR, Sinopharm Chemical Reagent Co., Ltd, Shanghai), and 5 mM DL-Dithiothreitol (DTT, 99%, Aladdin Industrial Corporation, Shanghai). Reduced nicotinamide adenine dinucleotide disodium salt (NADH Na_2, ≥98.0%), adenosine-5'-triphosphate, disodium salt, trihydrate (ATP×Na_2, ≥98.0%) and fluorescein isothiocyanate isomer I (FITC, ≥90%, HPLC) were purchased from Beijing Solarbio Technology Co., Ltd. Albumin (98%, from bovine serum) was from J&K Scientific Ltd., Beijing. Other major reagents were provided by Sigma-Aldrich, such as D-ribulose 1,5-bisphosphate sodium salt hydrate (RuBP, ~90%), D-ribulose 1,5-diphosphate carboxylase (RuBisCO, from spinach partially purified powder, 0.02 unit/mg solid), D-(−)-3-Phosphoglyceric acid disodium salt, ⩾93% (3-PGA), glyceraldehyde 3-phosphate dehydrogenase (GAPDH, from rabbit muscle lyophilized powder), 3-phosphoglyceric phosphokinase (PGK, from baker's yeast (*S. cerevisiae*), ammonium sulfate suspension, ≥1000 units/mg protein), Glycerol 3-phosphate Oxidase (G3POX, from *Pediococcus* sp. lyophilized powder), α-glycerophosphate dehydrogenase (G3PDH, from rabbit muscle, type I, ammonium sulfate suspension), triosephosphate isomerase (TPI, from baker's yeast (*S. cerevisiae*), ammonium sulfate suspension) and catalase (from bovine liver powder). All the chemicals were used as received.

2.2. Fabrication of PMRs

The PMRs were fabricated by sealing one molded PDMS layer having the microchannel pattern against another flat PDMS layer on top. The molded layer was made by using the standard soft photolithography technique[39] with the Sylgard 184 elastomer kit (Dow Corning Corporation) and the SU-8 mold (SU-8 50, MicroChem Crop.). The fabrication procedures are shown in Figure S1, and the three-dimensional structure of the fabricated microfluidic reactor can be seen in Figure 1(b). Standard soft photolithography includes design of microfluidic channels (mask design), fabrication of microfluidic mold by photolithography, molding and then bonding of the microfluidic chips (see Section S1 in Supplementary Information). Two methods were applied to bond the PMRs in order to fabricate two types of inner surfaces, the hydrophilic and the hydrophobic (Step 4 in Figure S1). The hydrophilic microfluidic reactors were sealed by the traditional plasma bonding method. 30 seconds of oxygen plasma (Harrick Plasma, USA) was applied to both the molded PDMS and the flat PDMS slice at the same time. They were then immediately bonded together. The reactors with hydrophobic inner surfaces were fabricated by direct bonding. One full-cured PDMS slice was made with the SU-8 mold after 30 min baking at 85 °C. One half-cured PDMS slice was made with a flat silicon wafer after 7 min baking at 85 °C. The cured molded PDMS was peeled off from the mold and gently placed onto the half-cured flat PDMS slice. After another 30 min of baking at 85 °C, the two slices were finally bonded together. The photograph of the fabricated PMRs can be seen in Figure 1(c). The height of the microchannels is 40 μm and the detailed dimensional information of the microchannels is shown in Figure S2.

2.3. Immobilization of RuBisCO

Increased concentrations of RuBisCO (0.5 to 4 μg μL^{-1}) in the reaction buffer were injected into the PMRs at the flow rate of 2.5 μL min^{-1} for different immobilization times (1 h to 6 h). After that, 100 μL reaction buffer was used to rinse the microreactors at the same flow rate. RuBisCO was then immobilized on the PDMS surface by physical adsorption and the RI-PMRs were ready for use (see Figure 1). The rinsed-out RuBisCO solutions were carefully collected to determine the protein-loading amount by calculating the protein concentration difference between the initially injected solution and the rinsed-out RuBisCO solution. The protein concentration was qualified by the Bradford method[40] using the Quick Start Bradford Protein Assay kit (Bio-Rad Pacific Ltd.), which was determined by measuring the absorbance at the wavelength of 595 nm using a UV-visible spectrometer (UV2450, Shimadzu). Different BSA solutions (0.125 – 1 mg mL^{-1}) were selected as standards to plot the calibration curve (see Figure S3). The protein-loading amount of the immobilization method was calculated by

$$\text{protein-loading amount } (\mu g) = C_0 V_i - C_1 V_w \quad (1)$$

where C_0 is the protein concentration of initially injected RuBisCO solution (μg μL^{-1}), C_1 is the protein concentration of the rinsed-out RuBisCO solution (μg μL^{-1}), V_i is the volume of initially injected RuBisCO solution (μL), V_w is the volume of washed solution collected from the outlet of the reactor (μL). The protein loading amounts of different RI-PMRs were recorded to find the optimal fabrication condition.

2.4. Surface characterization of RI-PMRs

The surface characterization of the inner surfaces of the PMRs and RI-PMRs was conducted by scanning electron microscope (SEM, JEOL JSM6490), the standard contact angle goniometer (Model 200, Ramé-Hart Instrument Co.), an attenuated total reflection Fourier transform infrared spectroscopy (ATR-FTIR, Bruker Vertex-70) and fluorescence microscope (Olympus BX41) to confirm the immobilization of RuBisCO. Circular dichroism (CD) spectrophotometer (JASCO J-1500) was also

used to study the secondary structure changes of RuBisCO after immobilization.

2.5. Assay of RuBisCO activity

The activities of the immobilized RuBisCO were determined using the amplification signal assay adapted from the previously reported method.[16, 41] The detailed procedures are shown in Section S2 of Supplementary Information. Generally, the reactant mixture (66 mM HCO_3^- and 0.5 mM RuBP in the reaction buffer) was passed through the RI-PMRs at the flow rate of 7 μL min^{-1} (here the reaction time is 1 min). The production solution (the mixture of RuBisCO, RuBP, HCO_3^- and the products in the reaction buffer) was collected from the outlet of the reactors before it was added into the assay mixture to determine the amount of 3-PGA. The composition of the assay mixture is listed in Section S2 of the Supplementary Information. Then, the 3-PGA amount in the production solutions could be determined from the calibration line generated by adding different amounts of standard 3-PGA dissolved in the reaction buffer into the assay mixture (see Figure S4). The RuBisCO activity was accordingly defined as the production rate of 3-PGA (μmol g^{-1} RuBisCO min^{-1}).

2.6. Kinetic study of RI-PMRs

Kinetic parameters are important indicators to evaluate the enzyme immobilization method. Here, different concentrations of RuBP (0.01 mM – 2 mM) and 66 mM HCO_3^- in reaction buffer were flowed through the RI-PMRs for RuBisCO activity evaluation. The RuBisCO activities under different concentrations of RuBP were fit to a Michaelis–Menten-type model using the hyperbola regression by GraphPad Prism 7 to derive the maximal reaction rate (V_{max}) and the Michaelis-Menten constant (K_m) parameters of the immobilized RuBisCO.

2.7. Feasibility of 3-PGA generation by RI-PMRs

The feasibility of producing 3-PGA using the RI-PMRs was examined by injecting 0.5 mM RuBP and 66 mM HCO_3^- in the reaction buffer through the as-prepared RI-PMRs using a syringe pump. The production solution was collected from the outlet to determine the 3-PGA amount (nmol) with the amplification signal assay. The injection flow rate was adjusted from 7 μL min^{-1} to 0.35 μL min^{-1}, causing the reaction time to increase from 1 min to 20 min (Section S3 in Supplementary Information). Then the feasibility could be evaluated by checking whether the 3-PGA production increased with the increased reaction time. Control experiments were also conducted at the same time with the PMRs that the same amount of BSA was immobilized in the same conditions (BI-PMRs).

2.8. Thermal stability of RI-PMRs

To test the thermal stability of the RI-PMRs, several prepared RI-PMRs were first incubated in the oven at different temperatures (from 20 to 70 °C) for 10 min and then the RuBisCO activities of each RI-PMRs were examined. RI-PMRs were also incubated at 50 °C for up to 60 min to examine their stability at elevated temperature for a prolonged time. The largest RuBisCO activity (A_t) was normalized to 100% and the relative RuBisCO activities at different incubation temperatures and incubation times were calculated as a percentage of A_t. Thermal stability of free RuBisCO was tested at the same condition for comparison as seen in our precious work.[16]

2.9. Reusing and refreshing of RI-PMRs for 3-PGA production

Reusing the RI-PMRs means one RI-PMR being used repeatedly. It was evaluated by continuously injecting 0.5 mM RuBP and 66 mM HCO_3^- in the reaction buffer through the same reactor to produce 3-PGA for several cycles. Every 21 μL of production solution collected at the outlet refers to one cycle of reuse. The RuBisCO activity was measured from the collected production solution for each cycle of reuse. The relative RuBisCO activities were calculated as a percentage of the initial RuBisCO activity in the first cycle.

Taking account of the reversible feature of physical adsorption, the RI-PMRs are likely to be washed off and then re-immobilized with new RuBisCO. This is defined as the refreshing of the RI-PMRs. The washing of the RI-PMRs was achieved by injecting the 50 mM citric acid/sodium citrate buffer (pH 3.0) at 7 μL min^{-1} for 3 h followed by injecting DI water to remove the residual acid buffer. The RI-PMRs was then dried in the oven at 60 °C overnight before the immobilization of new RuBisCO. One reactor was examined for several cycles of refreshing. One cycle of refreshing included the tests of flowing fresh 21 μL of reactant mixture solution through the RI-PMRs for the 3-PGA production after both the new immobilization and the washing of RuBisCO. The RuBisCO activity was measured from the collected production solution for each cycle of refreshing. The relative RuBisCO activities were calculated as a percentage of the initial activity of a newly prepared RI-PMR.

2.10. Continuous production of 3-PGA from RI-PMRs and reactors scaling out

Continuous production of 3-PGA was achieved by constantly injecting the reactant mixture (from 21 to 1680 μL) into the RI-PMRs at the flow rate of 7 μL min^{-1} to examine their 3-PGA production ability in lab-scale. Then the RI-PMRs were refreshed with new immobilized RuBisCO and continued to inject the reactant mixture for 3-PGA production. The refreshing was conducted for two times, bringing the production solution volume up to 5 mL.

Regarding the large-scale synthesis in future applications, the RI-PMRs were assessed by scaling out from one reactor to two parallel reactors and six parallel reactors as a proof-of-concept. The reactant mixture was injected into the parallel reactors at the same flow rate (7 μL min^{-1}) simultaneously. Then the production solutions were collected together for the future 3-PGA amount determination.

3. Results and discussion

3.1. Comparison of the pristine PMR and the plasma-treated PMR in RuBisCO immobilization

RuBisCO in the reaction buffer (1 μg μL^{-1}) were injected into the pristine PMR and the plasma-treated PMR for 4 hours at the same time. At first, the SEM images and the water contact angles of the two types of PMRs before and after the RuBisCO immobilization were characterized to compare their protein

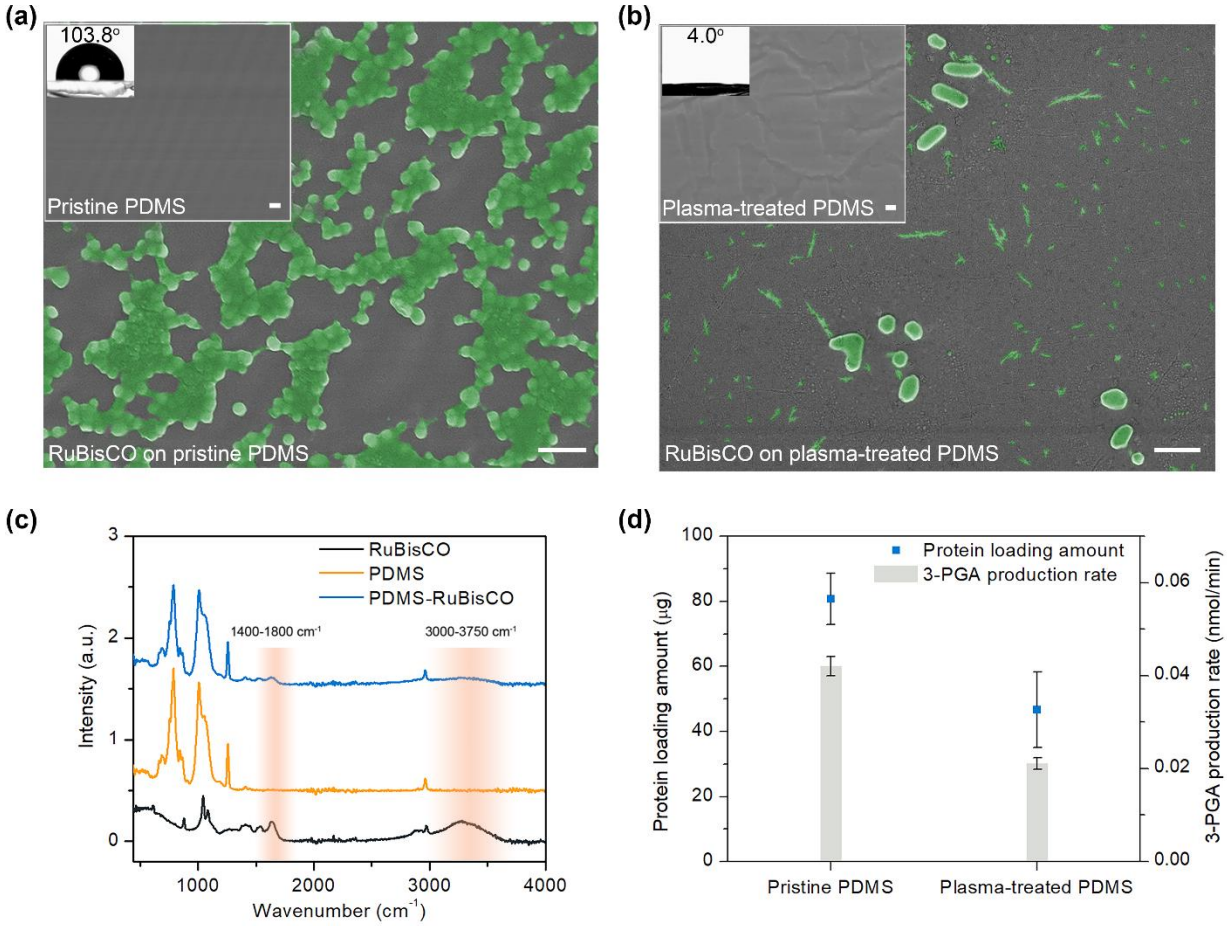

Figure 2. Comparison of the pristine PMRs and the plasma-treated PMRs in the RuBisCO immobilization. (a) and (b) are the SEM images of the inner surfaces of RuBisCO-immobilized pristine PMRs and RuBisCO-immobilized plasma-treated PMRs, respectively. The inset of (a) is the pristine PDMS surface before immobilization and the inset of (b) is the plasma-treated PDMS surface before immobilization. The scale bars are 1 μm. The sideview images of water drops on the pristine PDMS and the plasma-treated PDMS are shown on the top left of the insets. The measured water contact angles are 103.8° ± 1.1° and 4.0° ± 0.6°, respectively. (c) ATR-FTIR spectrum of RuBisCO (dark line), PDMS (yellow line) and the RuBisCO immobilized PDMS microchannels (PDMS-RuBisCO, blue line). New peaks (1400 – 1800 cm^{-1} and 3000 – 3750 cm^{-1}) were observed after the RuBisCO immobilization when compared with the pristine PDMS microfluidic channels. (d) Comparison of the protein loading amounts and the RuBisCO activities of the pristine PMRs and plasma-treated PMRs. The RuBisCO concentration is 1 μg $μL^{-1}$ with the immobilization time of 4 h. 0.5 mM RuBP and 66 mM HCO_3^- are injected at the flow rate of 7 μL min^{-1} with the reaction time of 1 min. All data are presented as mean ± s.d. (n = 3).

loading abilities. The SEM images of the inner surfaces of both the pristine PMRs and the plasma-treated PMRs are presented in Figure 2 (a) and (b). The inner surfaces of the pristine PMR before the RuBisCO immobilization were smooth and flat (see the inset of Figure 2 (a)). In contrast, some wrinkles were already present on the inner surfaces of the plasma-treated PMR (see the inset of Figure 2 (b)), which may be caused by the prolonged plasma treatment.[42] As shown by the water contact angle results on the top left of the insets, the pristine PDMS is highly hydrophobic (water contact angle is 103.8° ± 1.1°) whereas the plasma treatment makes it highly hydrophilic (water contact angle is 4.0° ± 0.6°). After the RuBisCO immobilization, some particles were observed on the inner surfaces of both types of PMRs (green particles in Figure 2 (a) and (b)). These particles indicated the immobilized and aggregated RuBisCO.

The immobilization of RuBisCO can also be confirmed by the measurements of ATR-FTIR spectrum of the microfluidic channels (Figure 2 (c)). New peaks (1400 – 1800 cm^{-1} and 3000 – 3750 cm^{-1}) were observed after the RuBisCO immobilization when compared with the pristine PDMS microfluidic channels. Particularly, the FTIR spectrum of the RI-PMRs has a weak band at about 1600 cm^{-1}, which could be referred to the vibrational modes of the peptide bonds (amide bands). This absorption band confirms the effective RuBisCO immobilization. The fluorescence images in Figure S5 also confirms the successful immobilization of RuBisCO.

Notably, much denser RuBisCO particles are observed on Figure 2(a) than Figure 2(b), suggesting that more RuBisCO are immobilized on the pristine PMR than on the plasma-treated PMRs. However, RuBisCO may coat on the surface as a thin layer, which prevents us from accurately observing by SEM. Therefore, the specific protein-loading amounts of the pristine and the plasma-treated PMRs should be investigated. As shown by the blue squares in Figure 2(d), the pristine PMR immobilized larger protein loading amount (~ 80.7 μg) than the plasma-treated PMR did (~ 46.7 μg). The protein loading efficiency for the pristine PMR (~23.4%) is also higher than that for the plasma-treated one (~8.6%), but lower than that by chemical immobilization (~50%).[16] Accordingly, the 3-PGA production

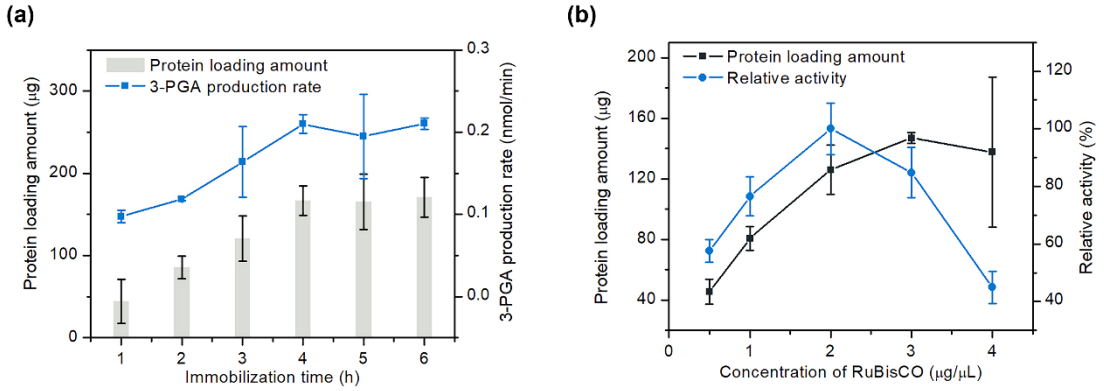

Figure 3. Investigation of the RuBisCO immobilization conditions. (a) Protein loading amounts and RuBisCO activities as a function of the immobilization time, showing that both the protein loading amount and the 3-PGA production rate increase with longer immobilization time and then saturate after 4 h. Here the RuBisCO concentration is 2 μg μL^{-1}. In experiment, 0.5 mM RuBP and 66 mM HCO_3^- are injected at the flow rate of 7 μL min^{-1}. (b) Protein-loading amount and the relative RuBisCO activity as a function of the concentration of the injected RuBisCO, showing that the protein loading amount reaches maximum at 3 μg μL^{-1} while the relative activity peaks at 2 μg μL^{-1}. The immobilization time is kept constant at 4 h, and 0.5 mM RuBP and 66 mM HCO_3^- are injected at the flow rate of 7 μL min^{-1}. All data are presented as mean ± s.d. (n = 3). Based on (a) and (b), the optimal conditions are chosen to be 4 h for the immobilization time and 2 μg μL^{-1} for the RuBisCO concentration.

rate (RuBisCO activity) of the pristine PMR (0.04 nmol min^{-1}) is about 2 folds of that of the plasma-treated PMRs (0.02 nmol min^{-1}), as seen from the grey bars in Figure 2(d). On the whole, it is verified that RuBisCO can be immobilized on PDMS by physical adsorption and the hydrophobic surface can immobilize more RuBisCO than the hydrophilic surface. The physical adsorption method eliminates the use of additional chemical likers, making the experimental process simple and green.

It has been reported that the enzymes in aqueous solutions are more likely to be adsorbed on the hydrophobic surfaces.[43] The interaction forces between the enzyme and the PDMS surface are mainly physical forces including van der Waals electrostatic interactions, hydrophobic interactions, Coulombic forces, hydrogen bonds and so on.[28, 44] The experimental results here prove that the hydrophobicity plays a significant role in the enzyme immobilization. The hydrophobic interaction would increase the immobilization amount of enzyme[23] and then improve the 3-PGA production rate. Therefore, in the following studies, the pristine PMR is used for the RuBisCO immobilization.

3.2. Optimal conditions investigation for RuBisCO immobilization on PMRs

The immobilization conditions were investigated in the aspects of the immobilization time and the enzyme concentration. When 2 μg μL^{-1} of RuBisCO was injected into the PMRs at the flow rate of 2.5 μL min^{-1} for an increased time (from 1 to 4 h), the protein loading amount of PMRs was increased by ~ 3.8 folds (from 44.5 to 171 μg), as shown by the grey bars in Figure 3(a). Correspondingly, the 3-PGA production rate was also increased from 0.10 to 0.21 nmol min^{-1} as the immobilization time increased (see the blue squares in Figure 3(a)). In brief, a longer immobilization time results in a larger amount of RuBisCO immobilized onto the PMRs inner surface, therefore causing a larger 3-PGA production. However, when the immobilization time continued to increase from 4 h to 5 h and then 6 h, the protein loading amount and the 3-PGA production rate tended to saturate. This may be due to the limited space of the PMRs for RuBisCO immobilization, which leads to the saturations of protein loading amount and thus 3-PGA production rate. Therefore, the immobilization time of 4 h is sufficiently long for protein loading and used as the working condition for further tests. Compared with the chemical immobilization method which often needs almost two days, the procedures of physical immobilization only take several hours, greatly reducing the fabrication time.

Next, the concentration of RuBisCO was also adjusted from 0.5 to 4 μg μL^{-1} to examine its influence on the protein-loading amount and the production rate. As shown in the dark squares of Figure 3(b), the protein-loading amount goes up with the increase of RuBisCO concentration and tends to saturate when the RuBisCO concentration goes up to 3 μg μL^{-1}. It may be ascribed to the saturation of the available PMRs surfaces for the RuBisCO immobilization. Similarly, the RuBisCO activity is also increased with the increasing RuBisCO concentration (blue circles in Figure 3(b)). But the activity reaches its maximum at the RuBisCO concentration of 2 μg μL^{-1} and then drops rapidly with the further increase of the RuBisCO concentration. Since RuBisCO is immobilized on the inner surfaces of PMRs by the physical adsorption, if the surfaces are already fully covered by one layer of RuBisCO, additional RuBisCO would aggregate into multiple layers. The active sites of RuBisCO may be covered by the additional layers and the supports, leading to the steric hindrance. The additional RuBisCO may also be easily rinsed out when the reactant runs through the reactor, causing a reduction of the enzyme activity. Then, the RuBisCO concentration 2 μg μL^{-1} and the immobilization time 4 h were chosen as the optimal conditions for the following RI-PMRs preparation to balance the protein loading amount and the RuBisCO activity.

3.3. Kinetics study of RI-PMRs

Next, the kinetic parameters of the immobilized RuBisCO were experimentally determined (see Figure 4(a)). As listed in Table S1, the RI-PMRs have K_m = 0.090 mM and V_{max} = 0.008 mmol min^{-1} g^{-1} RuBisCO. Compared with the free RuBisCO, which has K_m = 0.049 mM and V_{max} = 0.169 mmol min^{-1} g^{-1} RuBisCO, the RI-PMRs has a relatively higher K_m (see Table

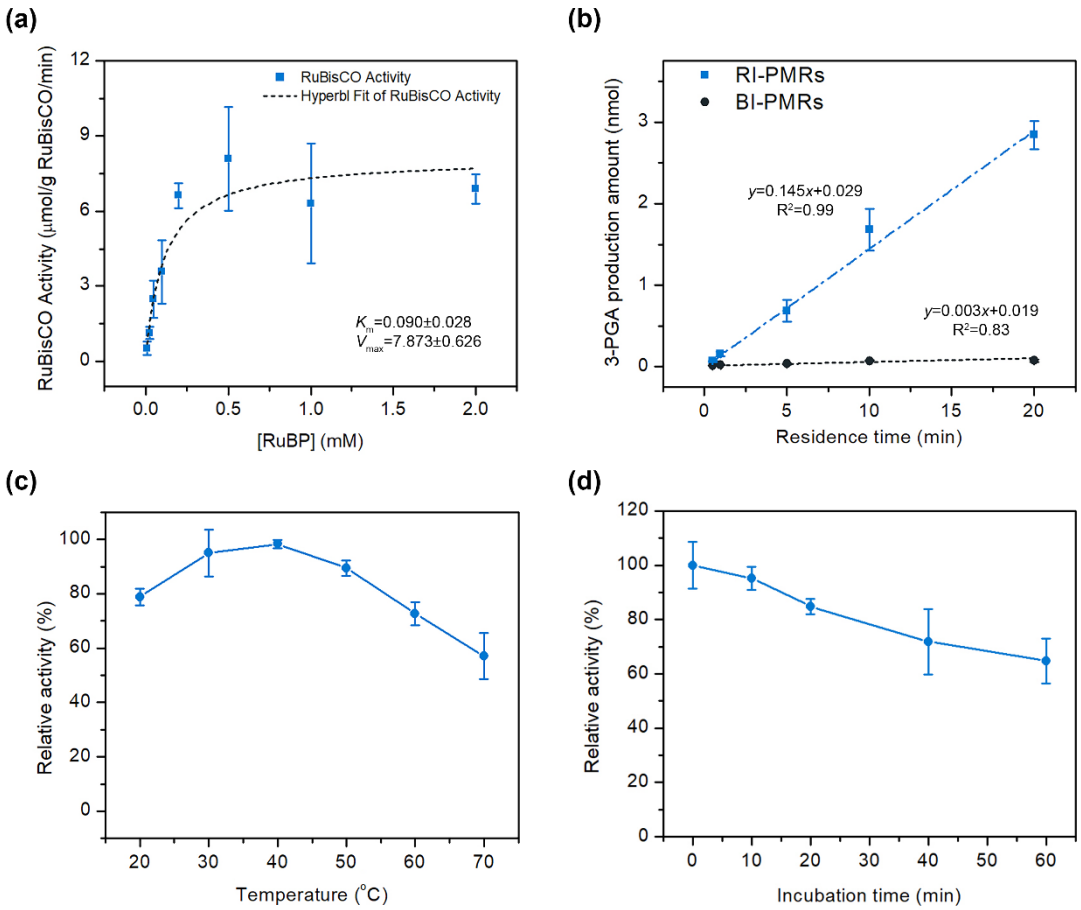

Figure 4. Measured performances of the RI-PMRs. (a) Kinetics parameters of the physically-immobilized RuBisCO. Blue squares are the RuBisCO activities at different concentration of RuBP. The collected production solutions are 100 μL. The RuBP concentrations are 0.025 – 2 mM for the RI-PMRs reaction. The concentration of bicarbonate (HCO_3^-) in the reaction buffer is 66 mM. K_m and V_{max} values are calculated by the GraphPad Prism 7 according to the hyperbola regression fitting of Michaelis–Menten model. The hyperbola regression fitting line is shown in dark dotted curve. (b) Production of 3-PGA using the RI-PMRs and BI-PMRs. Blue squares are the 3-PGA amounts produced by the RI-PMRs as a function of the residence time, dark circles are the 3-PGA amounts produced by the BI-PMRs (as the control). The RI-PMRs are made under the optimal conditions (the RuBisCO concentration of 2 μg μL^{-1} and the immobilization time of 4 h). The BI-PMRs are fabricated by 4 h immobilization of 2 μg μL^{-1} of BSA. 0.5 mM RuBP and 66 mM HCO_3^- are injected at different flow rates to control the reaction time. (c) Thermal stability of immobilized RuBisCO. Blue circles show the relative activities of the immobilized RuBisCO retained after incubation of 10 min at different temperatures (20 – 70 °C). All samples are incubated for 10 min before the activity assay. (d) Relative activities of the immobilized RuBisCO retained after a prolonged incubation time up to 60 min at 50 °C (blue circles). The concentration is 0.5 mM for RuBP and 66 mM for HCO_3^-. The collected production solutions are 100 μL. Error bars represent the standard deviations from three independent experiments.

S1). This infers that the physical immobilization lowers the affinity of the immobilized enzyme for the reactant. It is mainly due to the steric hindrance of some active sites caused by the support, which is barely avoided after the enzyme immobilization.[45] From Table S1, the RI-PMRs also exhibits a lower V_{max} than the free RuBisCO. The reduction of activity is ascribed to the irreversible conformational changes of RuBisCO after immobilization.[46] It is also confirmed by the ATR-FTIR and CD spectra analysis as shown in Sections S5 and S6 of Supplementary Information. The chemical immobilization has the kinetic parameters K_m = 0.070 mM and V_{max} = 0.070 mmol min^{-1} g^{-1} RuBisCO (see Table S1). It is seen that the physically-immobilized RuBisCO has a slightly higher K_m than the chemically-immobilized RuBisCO has but a smaller V_{max} value. Compared with the chemical immobilization, the physical adsorption is inferior in the enzyme activity. It may be due to the formation of multiple layers of enzymes on the microchannel's surfaces after the physical immobilization by the continuous injection of RuBisCO for several hours. The coverage of the multi-layered enzyme may block the active sites of the inner enzyme from contacting the substrate, therefore reducing the specific enzyme activity.[47] In contrast, only one layer of enzyme would be formed when RuBisCO was chemically immobilized by static reaction in our previous study.[16]

3.4. Feasibility of RI-PMRs for 3-PGA production

After the RI-PMRs were prepared using the optimal conditions (i.e., 2 μg μL^{-1} of RuBisCO solution injected at 2.5 μL min^{-1} for 4 h), the feasibility of the as-prepared RI-PMRs was studied by injecting RuBP and HCO_3^- at different flow rates to produce 3-PGA with varying reaction times. As shown by the blue squares in Figure 4(b), the 3-PGA amount produced by RI-PMRs increased with longer reaction time. The RI-PMRs demonstrated a 3-PGA production rate at ~ 0.145 ± 0.008 nmol min^{-1} when the reaction time is less than 20 min (see the blue dash-dotted fitting line in Figure 4(b)). But when bovine serum (BSA) is immobilized onto the microfluidic reactors (BI-PMRs) as the control experiment, the 3-PGA production is hardly observed (the dark circles in Figure 4(b)). And the R^2 coefficient

of determination (0.83) indicates that the liner regression predictions of 3-PGA production amounts by BI-PMRs do not fit well with the experimental data (the dark dash fitting line in Figure 4(b)). It can therefore be inferred that the detected extremely small amount of 3-PGA may be the background noise during the experiments. Although the 3-PGA production rate by RI-PMRs is still lower than that by the microreactors with chemically-immobilized RuBisCO (see Table S4), it is still well proved that the glucose precursor, 3-PGA, can be successfully synthesized with the RI-PMRs by implementing the light-independent reactions pathway. In addition, the adjustment of reaction time can be achieved by simply controlling the injection flow rate of the reactant mixture.[48] Moreover, the flushing out of products in real time makes the production collection quite facile, and meanwhile greatly helps eliminate additional steps for enzyme inactivation and separation.[49]

3.5. Thermal stabilities of physically-immobilized RI-PMRs

Figure 4(c) and (d) show the influence of temperature on the stability of RuBisCO. In Figure 4(c), the highest activity of immobilized RuBisCO appears at 40 °C. And the optimal incubation temperature range (i.e., the temperature range that over 98% of maximum activity is retained after incubation) of RuBisCO shifts from 24 – 34 °C (free RuBisCO)[16] to 33 – 42 °C after the physical immobilization. But, compared with the chemical immobilization we investigated previously,[16] the optimal incubation temperature range becomes smaller. It is also worth noting that the immobilized RuBisCO retains 57% of activity at 70 °C. Although it is slightly lower than that of the chemically-immobilized RuBisCO (67%), it is still 5.7 times of that of the free RuBisCO (10%)[16] (see Table S4). When incubated at 50 °C for a long time up to 60 min (see Figure 4(d)), the physically-immobilized RuBisCO retains 65% of activity while the chemically-immobilized and the free RuBisCO retains 75% and 46%, respectively. These show that either the physical or the chemical immobilization can significantly enhance the resistance of RuBisCO to the thermal inactivation as compared to the free solution, and the physical immobilization has similar thermal stability with the chemical immobilization (i.e., 57% versus 67%). The improved thermal stability of RuBisCO is ascribed to the enhanced stability of the enzyme conformation after the physical adsorption. The immobilization technique offers multiple anchors on the support to fix the enzyme, which helps preserve the enzyme structure and the active sites. Nevertheless, due to the weaker attractive forces between the supports and the physically-immobilized enzyme, it is reasonable that the thermal stability is a bit lower than that of the chemically-immobilized enzyme. However, as shown in Figure S8, there are much more hydrophobic sites of RuBisCO than its covalent binding sites.[50] Although thermal effects make hydrophobic bonds easier to release than covalent bonds, a large number of hydrophobic sites help stabilize the enzyme, thereby reducing the difference between the two methods in terms of thermal stability.

3.6. Reusability of physically-immobilized RI-PMRs for 3-PGA production

Excellent reusability of enzyme is essential for industrial applications. As shown by the light blue bars in Figure 5(a), only 40% of the initial activity is maintained after ten cycles of reuse when the reaction time is 1 min (the corresponding injection flow rate is 7 μL min^{-1}). The reusability is relatively weakened compared with the chemically-immobilized RuBisCO (74% for 10 cycles). The activity loss may be due to the enzyme deactivation and detachment after the repeated uses and the flushing by the running reactant mixture.[51] Since the forces that take effect in physical immobilization are mostly van der Waals forces, electrostatic force and hydrogen bonds, the enzyme are more likely to desorb during the reactions compared with the chemically-immobilized enzyme, especially in the microfluidic processes that have strong shear forces between the fluid and the microchannels' surfaces.[30, 31] As shown in Figure S9, the enzyme deactivation may be the main reason to the activity loss. And compared with the chemically-immobilized enzyme, the enzymes after physical immobilization are more likely to be inactivated during long time reusing. In this situation, the physical adsorption may be not strong enough to immobilize the enzyme for the microfluidics applications. Hence, a stronger

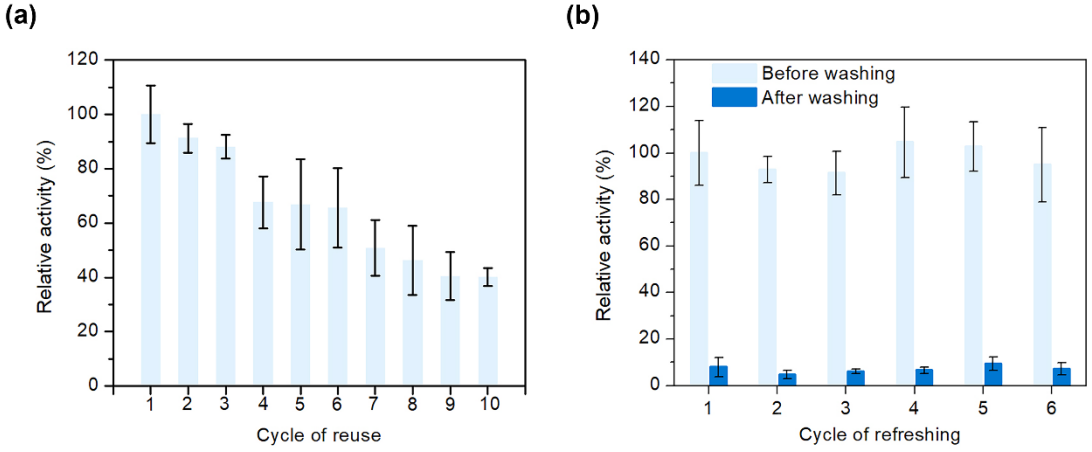

Figure 5. Reusing and refreshing of the RI-PMRs. (a) Reusing of the RI-PMRs, showing that the relative activity drops to 40% after 10 cycles of reuse. RuBP and HCO_3^- are flowed through the RI-PMR continuously. (b) Refreshing of the RI-PMRs, showing low activity (maximum 10%) after every time of washing (dark blue bars) and well restored activity (minimum 95%) after every time of new immobilization of RuBisCO (light blue bars). The RI-PMRs are prepared with RuBisCO of 2 μg $μL^{-1}$ and the immobilization time of 4 h. 0.5 mM RuBP and 66 mM HCO_3^- are injected at the flow rate of 7 μL min^{-1}.

immobilization method should be developed in future. However, the reusability experiment here proves the ease of reusing RuBisCO in the RI-PMRs by simultaneously pumping out the production solution and injecting new reactant mixture. Since RuBisCO is quite precious and costly, it also proves the necessity of immobilizing RuBisCO in the microfluidic reactors for the glucose precursor production.

3.7. Refreshing of the RI-PMRs for 3-PGA production

Although the reusability of RI-PMRs is not very good, they could be refreshed by washing and immobilizing new RuBisCO due to the reversibility of physical adsorption. The first light blue bar in Figure 5(b) shows the activity of a newly prepared RI-PMR. After being washed by the acid buffer, the activity of RI-PMR rapidly drop to nearly zero (the dark blue bars in Figure 5(b), maximum 10%). This indicates the efficient desorption of the immobilized RuBisCO by the flushing acid buffer. After the immobilization of new RuBisCO, the RuBisCO activity reaches minimum 95% of its initial activity after several cycles of refreshing (see the light blue bars in Figure 5(b)). Water contact angle analysis in Figure S10 shows that PDMS becomes hydrophilic after RuBisCO immobilization and recovers to hydrophobic after washing. This also shows that RuBisCO can be desorbed by the acid buffer rinsing and can then be well immobilized again on the PMRs, proving the reversibility of the physical adsorption method. On the whole, although the physically-immobilized enzyme is liable to desorb by physical forces (e.g., shear force of running flow) during reactions, the supports can be refreshed by a simple washing step. And then the refreshed supports are ready to immobilize new enzymes without affecting their activities, therefore saving the fabrication cost and time. It is then possible to replace and renew the immobilized enzymes and to perform different reactions by reusing the same reactor, making the biocatalytic process in microreactors reusable and sustainable. However, for the chemically immobilized RuBisCO reactor used in our previous study, the refreshing is not feasible. Every reactor can only be used for one time, which would cause a big waste in the large-scale industrial applications in the future. The non-specific adsorption property makes the physical immobilization method highly suitable for multi-enzymatic reactions, in which multiple enzymes need to be immobilized in different regions of a single reactor. More specifically, it well fits the cascaded multi-enzymatic steps of Calvin cycle for artificial synthesis of glucose using microfluidic reactors.

3.8. Continuous production of 3-PGA from RI-PMRs and reactors scaling out

When one reactor was used for the continuous production of 3-PGA, the production amount increased nonlinearly with the increasing volume of the injected reactant mixture, as shown by the blue squares in Figure 6. This was ascribed to the gradually decreased RuBisCO activity after repeated use and long operation time. For the first 1680 μL, 3.2 nmol of 3-PGA was produced. The total operation time (the time to collect a specific volume of products) is 4 h, determined by dividing the production volume by the flow rate. Then the reactor was refreshed with new immobilized RuBisCO. The activity of the reactor was recovered, and the production of 3-PGA was resumed to increase nonlinearly. The refreshing of the RI-PMRs was repeated two times to synthesize 3-PGA up to 5 mL, where 9.4 nmol of 3-PGA was produced. More refreshing times could be conducted to achieve larger production if needed. However, the recovery of the production by the microreactors with chemically immobilized RuBisCO was not implemented in our previous study.[16]

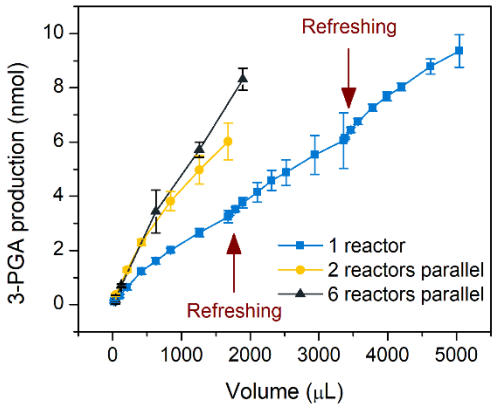

Figure 6. Continuous production of 3-PGA as a function of the volume of collected production solution. The RI-PMRs are prepared with RuBisCO of 2 μg μL^{-1} and the immobilization time of 4 h. 0.5 mM RuBP and 66 mM HCO_3^- are injected at the flow rate of 7 μL min^{-1}.

The RI-PMRs were also scaled out from one reactor to two parallel reactors and six parallel reactors to increase the production in a short operation time. As shown by the yellow circles in Figure 6, the production amount of 3-PGA by two parallel reactors also increases nonlinearly with the increasing amount of the injected RuBP. But the instantaneous reaction rate was obviously larger than that of one reactor. Here the instantaneous rate is the rate at which a reaction is proceeding at any specific time. The production of 3-PGA was improved to 6.0 nmol for 1680 μL of production solution, which is almost 2-fold of that by one reactor. And the operation time was reduced to 2 h (half of the operation time by one reactor). The 3-PGA production by six parallel reactors also increases nonlinearly, but the trend is closer to linear as compared to that of the two parallel reactors. A slightly larger instantaneous reaction rate is also observed when the injection volume is larger than 500 μL. The production of 3-PGA was further improved to 7.3 nmol for 1680 μL of production solution (2.2-fold of that by one reactor and 1.2-fold of that by two reactor). The operation time was impressively reduced to 40 min (one-sixth of that by one reactor). The increasing parallel reactors considerably help reduce the impact of poor reusability of one single reactor and save the operation time. Here the parallelization of two and six reactors is just a proof of concept of the large production. In future applications, tens and hundreds of RI-PMRs could be paralleled for even larger scale of 3-PGA production. Conveniently, the microfluidic reactor can also be scaled up to larger characteristic dimensions of channel and scaled out with the parallel reactor system for industrial applications. With such system, the large-scale synthesis of 3-PGA in short time would be potentially promising in future applications.

4. Conclusion

In this work, RuBisCO has been immobilized into two types of PMRs, the pristine (hydrophobic) and the plasma-treated (hydrophilic) ones. The hydrophobic PMRs showed a higher protein loading capacity and a larger activity retention than the hydrophilic PMRs. The RuBisCO concentration 2 μg μL^{-1} and the immobilization time 4 h were found to be the optimal conditions to maximize the protein loading amount and the RuBisCO activity for the RI-PMRs preparation. Compared with the chemical immobilization method, it is simple and fast. The RI-PMRs demonstrated its feasibility in 3-PGA production and obtained the production rate at 0.145 ± 0.008 nmol min^{-1} when the reaction time was $<$ 20 min. Compared with the free RuBisCO, the immobilized RuBisCO also presented a 5.7-fold thermal stability. But the RI-PMRs had a weak reusability, only retaining 40% of the initial activity after 10 cycles of reusing. In general, the physical immobilization measured inferior but similar performances (e.g., enzyme kinetics, production rate, thermal stability) as compared to the chemical immobilization due to the weak affinity of the physical adsorption. However, the physical immobilization has a special merit of reversibility, making it easy to release the used enzymes and to re-immobilize new enzymes on the same reactor. Experiments showed that the physically-immobilized RI-PMRs could restore at least 95% of activity after 5 cycles of refreshing. The non-specific adsorption property makes the physical immobilization method highly suitable for multi-enzymatic reactions in microreactors in a green and sustainable manner. It is possible to replace and renew the immobilized enzymes and then to perform different reactions by reusing the same reactor. Up to 5 mL of 3-PGA production was achieved by injecting the reactant mixture and refreshing the reactor. Scaling out from one reactor to two parallel reactors and six parallel reactors was also carried out as a proof-of-concept for the large-scale synthesis. The production of 3-PGA was improved by 2.2-fold for 1680 μL of production solution compared with one reactor and the operation time was greatly reduced.

It also allows to cascade multi-enzymatic steps in different regions of a single reactor, facilitating the artificial synthesis of glucose using Calvin cycle in the microfluidic reactors. Physical immobilization can be combined with chemical immobilization for future application to improve the performance of enzyme. The detailed comparisons of physical immobilization and free solution in this work, together with our previous study on chemical immobilization, build up comprehensive technical bases for the immobilization of enzymes in microfluidic reactors and the imitation of NPS in chloroplasts, which can be further used to artificially synthesize basic food materials (e.g., glucose precursor) for food crisis relief and future space colonization.

Conflicts of interest

There are no conflicts to declare.

Acknowledgements

This work is supported by Research Grants Council of Hong Kong (15221919, 15215620, and N_PolyU511/20), Hong Kong Polytechnic University (1-ZE14 and 1-ZVGH), Shandong Provincial Natural Science Foundation, China (ZR2016XJ004) and Doctoral cooperation fund of Shandong Academy of Sciences (2017BSHZ007). The technical assistance and facility support of the Materials Research Centre (MRC), the University Research Facility in Material Characterization and Device Fabrication (UMF) and the University Research Facility in Life Sciences (ULS) of the Hong Kong Polytechnic University are appreciated as well.

Notes and references

1 J. Barber and P. D. Tran, *J. Royal Soc. Interface*, 2013, **10**, 20120984.
2 P. H. McNeil and D. A. Walker, *Arch. Biochem. Biophys.*, 1981, **208**, 184-188.
3 A. Makino and B. Osmond, *Photosynth. Res.*, 1991, **29**, 79-85.
4 K. H. Suss, C. Arkona, R. Manteuffel and K. Adler, *Proc. Natl. Acad. Sci. U.S.A.*, 1993, **90**, 5514-5518.
5 K. H. Suss, I. Prokhorenko and K. Adler, *Plant Physiol.*, 1995, **107**, 1387-1397.
6 A. M. Kunjapur and R. B. Eldridge, *Ind. Eng. Chem. Res.*, 2010, **49**, 3516-3526.
7 J. S. Lee, S. H. Lee, J. H. Kim and C. B. Park, *Lab Chip*, 2011, **11**, 2309-2311.
8 X. Huang, J. Liu, Q. Yang, Y. Liu, Y. Zhu, T. Li, Y. H. Tsang and X. Zhang, *RSC Adv.*, 2016, **6**, 101974-101980.
9 T. E. Miller, T. Beneyton, T. Schwander, C. Diehl, M. Girault, R. McLean, T. Chotel, P. Claus, N. S. Cortina, J.-C. Baret and T. J. Erb, *Science*, 2020, **368**, 649-654.
10 J. J. Concepcion, R. L. House, J. M. Papanikolas and T. J. Meyer, *Proc. Natl. Acad. Sci. U.S.A.*, 2012, **109**, 15560-15564.
11 Y. Tachibana, L. Vayssieres and J. R. Durrant, *Nat. Photonics*, 2012, **6**, 511.
12 S. Chakrabarti, S. Bhattacharya and S. K. Bhattacharya, *Biotechnol. Bioeng.*, 2003, **81**, 705-711.
13 T. M. Hery, S. Satagopan, R. G. Northcutt, F. R. Tabita and V.-B. Sundaresan, *Smart Mater. Struct.*, 2016, **25**, 125033.
14 S. Satagopan, Y. Sun, J. R. Parquette and F. R. Tabita, *Biotechnol. Biofuels*, 2017, **10**, 175.
15 K. Lee, J. P. Evans, S. Satagopan, Y. Sun, J. R. Parquette, V. B. Sundaresan, F. R. Tabita and B. R. Bakshi, *ACS Sustain. Chem. Eng.*, 2020, **8**, 16833-16841.
16 Y. Zhu, Z. Huang, Q. Chen, Q. Wu, X. Huang, P.-K. So, L. Shao, Z. Yao, Y. Jia, Z. Li, W. Yu, Y. Yang, A. Jian, S. Sang, W. Zhang and X. Zhang, *Nat. Commun.*, 2019, **10**, 4049.
17 R. A. Sheldon and D. Brady, *ACS Sustain. Chem. Eng.*, 2021, **9**, 8032-8052.
18 Y. Zhu, Q. Chen, L. Shao, Y. Jia and X. Zhang, *React. Chem. Eng.*, 2020, **5**, 9-32.
19 C. Goldhahn, I. Burgert and M. Chanana, *Adv. Mater. Interfaces*, 2019, **6**, 1900437.
20 K. F. Lei, in *Microfluidics in Detection Science: Lab-on-a-chip Technologies*, ed. F. H. L. a. H. O. Fatoyinbo, The Royal Society of Chemistry, United Kingdom, 2014, vol. 5, ch. 1, pp. 1-28.
21 K. Y. Chumbimuni-Torres, R. E. Coronado, A. M. Mfuh, C. Castro-Guerrero, M. F. Silva, G. R. Negrete, R. Bizios and C. D. Garcia, *RSC Adv.*, 2011, **1**, 706-714.
22 J. Zhou, A. V. Ellis and N. H. Voelcker, *Electrophoresis*, 2010, **31**, 2-16.
23 X. Yu, J. Xiao and F. Dang, *Langmuir*, 2015, **31**, 5891-5898.
24 X. Ren, M. Bachman, C. Sims, G. Li and N. Allbritton, *J. Chromatogr. B Biomed. Appl.*, 2001, **762**, 117-125.

25 J. A. Vickers, M. M. Caulum and C. S. Henry, *Anal. Chem.*, 2006, **78**, 7446-7452.
26 B. Larson, S. Gillmor, J. Braun, L. Cruz-Barba, D. Savage, F. Denes and M. Lagally, *Langmuir*, 2013, **29**, 12990-12996.
27 S. H. Lee and E. Ruckenstein, *J. Colloid Interface Sci.*, 1988, **125**, 365-379.
28 S. Cao and B. Liu, *Macromol. Biosci.*, 2009, **9**, 361-368.
29 K. D. Caldwell, R. Axén, M. B. Wall and J. Porath, *Biotechnol. Bioeng.*, 1976, **18**, 1573-1588.
30 N. R. Mohamad, N. H. C. Marzuki, N. A. Buang, F. Huyop and R. A. Wahab, *Biotechnol. Biotechnol. Equip.*, 2015, **29**, 205-220.
31 T. Klotzbach, M. Watt, Y. Ansari and S. D. Minteer, *J. Membr. Sci.*, 2006, **282**, 276-283.
32 P. Kosaka, Y. Kawano, O. El Seoud and D. Petri, *Langmuir*, 2007, **23**, 12167-12173.
33 L. Chronopoulou, G. Kamel, C. Sparago, F. Bordi, S. Lupi, M. Diociaiuti and C. Palocci, *Soft Matter*, 2011, **7**, 2653-2662.
34 L. Huang and Z.-M. Cheng, *Chem. Eng. J.*, 2008, **144**, 103-109.
35 B. Bucur, A. F. Danet and J.-L. Marty, *Biosens. Bioelectron*, 2004, **20**, 217-225.
36 M. Kumakura and I. Kaetsu, *J. Appl. Polym. Sci.*, 1984, **29**, 2713-2718.
37 Y.-K. Cen, Y.-X. Liu, Y.-P. Xue and Y.-G. Zheng, *Adv. Synth. Catal.*, 2019, **361**, 5500-5515.
38 A. Sassolas, L. J. Blum and B. D. Leca-Bouvier, *Biotechnol. Adv.*, 2012, **30**, 489-511.
39 D. C. Duffy, J. C. McDonald, O. J. Schueller and G. M. Whitesides, *Anal. Chem.*, 1998, **70**, 4974-4984.
40 M. M. Bradford, *Anal. Biochem.*, 1976, **72**, 248-254.
41 R. SULPICE, H. TSCHOEP, M. VON KORFF, D. BÜSSIS, B. USADEL, M. HÖHNE, H. WITUCKA-WALL, T. ALTMANN, M. STITT and Y. GIBON, *Plant Cell Environ.*, 2007, **30**, 1163-1175.
42 H. J. Hettlich, F. Otterbach, C. Mittermayer, R. Kaufmann and D. Klee, *Biomaterials*, 1991, **12**, 521-524.
43 V. Bartzoka, M. R. McDermott and M. A. Brook, *Adv. Mater.*, 1999, **11**, 257-259.
44 S. Koutsopoulos, J. van der Oost and W. Norde, *Langmuir*, 2004, **20**, 6401-6406.
45 K. B. de Oliveira, K. L. Mischiatti, J. D. Fontana and B. H. de Oliveira, *J. Chromatogr. B*, 2014, **945-946**, 10-16.
46 C. A. Haynes and W. Norde, *Colloids Surf. B: Biointerfaces*, 1994, **2**, 517-566.
47 S. L. Hirsh, M. M. M. Bilek, N. J. Nosworthy, A. Kondyurin, C. G. dos Remedios and D. R. McKenzie, *Langmuir*, 2010, **26**, 14380-14388.
48 C. Hu, Y. Bai, M. Hou, Y. Wang, L. Wang, X. Cao, C.-W. Chan, H. Sun, W. Li, J. Ge and K. Ren, *Sci. Adv.*, 2020, **6**, eaax5785.
49 E. Magnan, I. Catarino, D. Paolucci-Jeanjean, L. Preziosi-Belloy and M.-P. Belleville, *J. Membr. Sci.*, 2004, **241**, 161-166.
50 H. Zhang, J. Luo, S. Li, Y. Wei and Y. Wan, *Langmuir*, 2018, **34**, 2585-2594.
51 C. Chao, J. Liu, J. Wang, Y. Zhang, B. Zhang, Y. Zhang, X. Xiang and R. Chen, *ACS Appl. Mater. Interfaces*, 2013, **5**, 10559-10564.